Supplement of:

Summertime and wintertime atmospheric processes of secondary aerosol in Beijing

Jing Duan[1,2,3], Ru-Jin Huang[1,2], Yongjie Li[4], Qi Chen[5], Yan Zheng[5], Yang Chen[6], Chunshui Lin[1,2], Haiyan Ni[1,2], Meng Wang[1,2], Jurgita Ovadnevaite[7], Darius Ceburnis[7], Chunying Chen[8], Douglas R. Worsnop[9], Thorsten Hoffmann[10], Colin O'Dowd[7], Junji Cao[1,2]

[1]State Key Laboratory of Loess and Quaternary Geology (SKLLQG) and Key Laboratory of Aerosol Chemistry & Physics (KLACP), Institute of Earth Environment, Chinese Academy of Sciences, Xi'an 710061, China

[2]CAS Center for Excellence in Quaternary Science and Global Change, Chinese Academy of Sciences, Xi'an 710061, China

[3]University of Chinese Academy of Sciences, Beijing 100049, China

[4]Department of Civil and Environmental Engineering, Faculty of Science and Technology, University of Macau, Taipa, Macau 999078, China

[5]State Key Joint Laboratory of Environmental Simulation and Pollution Control, College of Environmental Sciences and Engineering, Peking University, Beijing 100871, China

[6]Chongqing Institute of Green and Intelligent Technology, Chinese Academy of Sciences, Chongqing 400714, China

[7]School of Physics and Centre for Climate and Air Pollution Studies, Ryan Institute, National University of Ireland Galway, University Road, Galway, H91CF50, Ireland

[8]CAS Key Laboratory for Biological Effects of Nanomaterials and Nanosafety, National Centre for Nanoscience and Technology, Beijing 100191, China

[9]Aerodyne Research, Inc., Billerica, MA, USA

[10]Institute of Inorganic and Analytical Chemistry, Johannes Gutenberg University Mainz, Duesbergweg 10–14, Mainz 55128, Germany

Correspondence to: Ru-Jin Huang (rujin.huang@ieecas.cn) or Qi Chen (qichenpku@pku.edu.cn)

Section S1: Source apportionments for OA datasets

Separate OA source apportionments were conducted in summer and winter individually. According to the summer dataset, a range of solutions with three to five factors from unconstrained runs were first examined. As shown in Fig. S1, POA factors mixed seriously with SOA factors and identical source factors can't be resolved by PMF. There was a COA factor resolved in the 3-factor solution, while no clear HOA factor could be resolved and POA mixed seriously with SOA in factor 2, which may both contain HOA and OOA sources. No HOA could be resolved when increasing the factor numbers and the factor further split into non-meaningful profiles. Meanwhile, clear peaks in m/z 53 and m/z 82 were found in PMF solutions, indicating

that there was likely have isoprene-derived sources mixed in POA or OOA factors, thus 4 factors were selected for the reasonable PMF solution. In order to get better results, the ME-2 approach was further applied to direct the apportionment towards an environmentally-meaningful solution by introducing *a priori* information (profiles) for certain factors. We constrained the COA and HOA using profiles from our previous study (Wang et al, 2017) and constrained ISOOA profile from Budisulistiorini et al. (2013). To minimize the effect from non-local input profiles, the *a* value approach was used to adjust the input profiles to a certain extent.

Similarly, a range of solutions with two to eight factors from unconstrained runs were first examined in winter. Fig. S2 showed the PMF results of 5-factor, 6-factor and 7-factor. POA factors including HOA, COA, BBOA and CCOA could be resolved in PMF solutions, while there was serious mixture between each other and POA with OOA. In order to get better results, the ME-2 approach was further applied to direct the apportionment towards an environmentally-meaningful solution by introducing *a priori* information (profiles) for certain factors. We constrained the HOA, COA, CCOA and BBOA using profiles from our previous study (Wang et al, 2017). Also, to minimize the effect from non-local input profiles (for all primary factors), the *a* value approach was used to adjust the input profiles to a certain extent.

Finally, we tested ME-2 solutions and selected reasonable results based on the verification of the rationality of unconstrained factors, distinct mass spectra and time series, interpretable diurnal cycles and good correlations with external tracers for all factors both in summer and winter. The final profiles and time series of individual factor were averaged from these reasonable solutions and the standard deviations of intensities at each *m/z* was shown as error bars in Fig. S3. Four OA factors including HOA, COA, ISOOA and OOA were resolved during summer, while six factors including HOA, COA, BBOA, CCOA, LO-OOA and MO-OOA were identified during winter.

Section S2: OA sources

Primary OA

HOA was resolved in both summer and winter, which was dominated by typical hydrocarbon ion series of C_nH_{2n+1} and C_nH_{2n-1}, particularly m/z 41, 43, 55, 57, 69 and 71 (Canagaratna et al., 2004; Mohr et al., 2009; Ng et al., 2011). The time series of HOA in summer and winter were both tightly correlated with that of BC (R^2 = 0.62 and 0.78 in summer and winter, respectively), which is a primary emission tracer of incomplete combustion. The diurnal cycles of HOA were characterized by high concentrations during nighttime (Fig. S4), likely due to increased diesel fleets which are allowed in urban Beijing only at night (Elser et al, 2016; Sun et al., 2016).

COA was also resolved in both summer and winter. The spectra of COA in our study were characterized by prominent ion peaks at *m/z* 55 and *m/z* 57 with higher m/z 55/57 ratio of 2.4 in summer and 2.1 in winter respectively, which have been shown to be robust markers for COA (Mohr et al., 2012; Crippa et al., 2013; Elser et al., 2016). Consistently, the time series of COA were

correlated well with that of *m/z* 55 with R^2 = 0.72 and 0.66 during summer and winter respectively. Both the diurnal cycles of COA during summer and winter showed distinct peaks at lunch (12:00 LT) and dinner (20:00 LT) time.

BBOA and CCOA were only resolved in wintertime. The mass spectrum of BBOA showed prominent signals at m/z 60 ($C_2H_4O_2^+$) and 73 (95% of which is $C_3H_5O_2^+$), which are well known fragments of levoglucosan and mannosan produced from incomplete combustion and pyrolysis of cellulose and hemicelluloses from biomass burning (Alfarra et al., 2007; Lanz et al., 2007; Mohr et al., 2009). Consistently, the time series of BBOA correlated very well with that of m/z 60 (R^2 = 0.87). BBOA showed a clear diurnal cycle with higher concentration during nighttime than that in daytime. The mass spectrum of CCOA is characterized by prominent contributions of unsaturated hydrocarbons, particularly PAH-related ion peaks (e.g., 77, 91, and 115) (Dall'Osto et al., 2013; Hu et al., 2013). Strong correlation was found between the time series of CCOA and that of the external combustion tracer chloride with R^2 value of 0.73. Similar to BBOA, the mass concentration of CCOA during nighttime was much higher than that during daytime with the mass fraction increased from 10% in afternoon to 25% during night, further confirming the enhanced coal combustion emissions from domestic heating in wintertime nights.

Secondary OA

During summertime, an OOA factor dominated by high peak at m/z 44 (CO_2^+) with a f_{44}/f_{43} value of 3.2 was identified, The diurnal cycle of OOA showed an obvious peak in afternoon combined with the increasing mass fraction during the same period, and the time series of OOA correlated well with that of sulfate (R^2 = 0.6). Similar good correlations between OOA and sulfate were also observed in previous Beijing summer studies (Huang et al., 2010; Sun et al., 2010; Hu et al., 2016).

In addition to OOA, an ISOOA derived from isoprene-oxidation was resolved in summer Beijing. As shown in Fig.S3, the mass spectrum of ISOOA was characterized by distinct ion peaks at m/z 53 ($C_4H_5^+$) and m/z 82 ($C_5H_6O^+$), with correlation between the time series of ISOOA and m/z 82 (R^2 = 0.46). This ISOOA profile was consistent with that resolved from ACSM organic spectra based on field study during summertime in the southeastern US and demonstrated in lab chamber (Budisulistiorini et al., 2013; Hu et al., 2015; Xu et al., 2015). Meanwhile, the diurnal cycle of ISOOA displayed minor peaks in afternoon, likely due to the gas-phase photochemical processing during afternoon when temperature and photochemical activity are the highest in a day. Such diurnal behaviors are consistent with the T-dependence on isoprene photochemistry activities (Xu et al., 2015; Zhang et al., 2017).

In comparison, there was no ISOOA resolved during winter due to low temperature and less biogenic emission sources, whereas two secondary OA sources defined as LO-OOA and MO-OOA were identified. As shown in Fig. S3, LO-OOA and MO-OOA both showed high ratios of intensity at m/z 44 over that at m/z 43 in mass spectra (the $f_{44}/_{43}$ value of MO-OOA (8.6) was much higher

than that of LO-OOA (2.61)). However, their time series and diurnal cycles differed from each other greatly. The time series of LO-OOA was highly correlated with that of nitrate in the entire winter period with $R^2 = 0.80$, while the time series of MO-OOA had a good correlation ($R^2 = 0.71$) with that of sulfate. The diurnal cycles of LO-OOA showed a dominant increasing trend from 8:00 to 20:00 LT, meanwhile the mass fraction of LO-OOA increased during the same period in daytime, which was similar with that of nitrate (As shown in Fig. S4). In comparison, the diurnal cycles of both concentration and fraction of MO-OOA showed decreasing trend from 8:00 LT to 16:00 LT, which was consistent with that of sulfate and RH.

Section S3: Diurnal cycles of PM$_1$ species

The diurnal cycles of PM$_1$ species between summer and winter are shown in Fig. S4. OA was characterized by two peaks occurring around noon (12:00-13:00 LT) and the evening (19:00-22:00 LT) both in summer and winter. The peak in noon was larger in summer than that in winter, likely due to the stronger photochemical oxidation capacity in daytime during summer. The diurnal cycle of mass fraction of OA in summer was also more variable than that in winter with two obvious peaks in the noon and evening. BC and chloride also showed similar diurnal cycles in summer and winter because both are primary emissions, and their concentrations were much higher during night than during day in winter because enhanced emissions from residential heating activities. Compared to primary species, secondary species displayed largely different diurnal cycles between summer and winter. In summer, sulfate showed continuous increase from 8:00 LT to 17:00 LT, even in the afternoon at the highest planetary boundary layer height as reflected in the trough of OA, suggesting its efficient formation. However, there was no similar increasing peak in winter, yet decreased from 8:00 LT to 16:00 LT instead and higher concentration in nighttime than daytime was observed during winter. In comparison, nitrate showed contrary diurnal cycles with that of sulfate both in summer and winter. The diurnal cycle of nitrate displayed a peak in the morning and then decreased dramatically from 8:00 LT to 16:00 LT during summer, while increasing trend of nitrate during the same time (8:00-16:00 LT) was observed in winter. Consistently, dominant increase of the mass fraction of sulfate in afternoon was observed in summer while similar increase was found for nitrate fraction in winter. Associated with sulfate and nitrate, the diurnal cycles of ammonium were affected by both sulfate and nitrate formation mechanisms, which showed medium increasing trends in daytime both in summer and winter.

Table S1. A summary of submicron aerosol composition and OA factors from AMS/ACSM measurements in Beijing, China.

Season	Summer					Winter							
Date	Jun-Jul, 2008	3 Aug-15 Sep, 2011	Jul-Sep, 2011	29 Jul–29 Aug, 2012	1 Jul-19 Aug, 2015	Jan-Feb, 2008	22 Nov-22 Dec, 2010	Dec, 2011-Mar, 2012	21 Nov, 2011-20 Jan, 2012	Jan, 2013	23 Jan–2 Mar, 2013	17 Dec, 2013- 17 Jan, 2014	4 Dec, 2015 - 6 Feb, 2016
Ref.	Zhang et al., 2013	Hu et al., 2016	Sun et al., 2015, 2018	Hu et al., 2017	This study	Zhang et al., 2013	Hu et al., 2016	Sun et al., 2015, 2018	Sun et al., 2013	Zhang et al., 2014	Hu et al., 2017	Sun et al., 2016	This study
PM_1	94.0	77.9	61.6	37.6	41.0	73.5	69.5	58.7	66.8	94.0	81.7	64.1	63.2
SO_4^{2-}	24.8	22	10.6	9.7	7.5	11.4	8.7	7.7	9.4	19.6	17.4	9.4	7.6
NO_3^-	20.1	16.8	15.6	6.4	5.6	9.2	6.8	10.3	10.7	12.5	16.2	7.2	10.5
NH_4^+	13.7	13.7	10.5	5.4	5.7	6.4	7.7	8.1	8.7	8.9	11.7	5.4	7.4
Cl^-	1.56	1.0	0.8	0.4	0.2	3.5	5.8	3.0	3.3	3.6	2.8	4.0	3.1
BC	-	4.4		3.2	2.9		6.0				3.9		3.4
FFOA			1.45					5.6					
HOA	13.5	3.4		1.4	1.5	33	4.2		5.9	5.4	5.5	3.9	3.6
COA		5.5	2.6	2.5	3.4		5.7	4.0	6.6	9.8	4.3	6.7	6.3
CCOA							7.2		11.4	9.3	5.0	7.6	6.1
BBOA			1.55				3.6	3.2				2.2	2.8
SV-OOA										12.8		12.1	
LV-OOA										13.8		4.4	
LO-OOA		9.7	4.3	5.3			5.4	5.5			5.0		7.1
MO-OOA		7.4	5.6	3.3			3.9	11.4			9.8		5.1
OOA	20.3				13.0	10			10.8				
ISOOA					1.0								
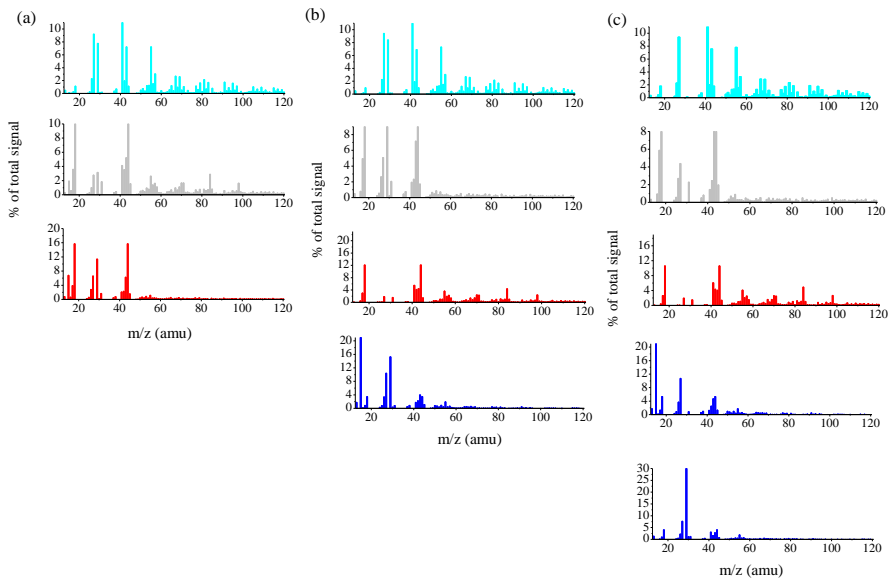
Figure S1. PMF profiles of OA sources for 3, 4 and 5 factor solutions during summer.
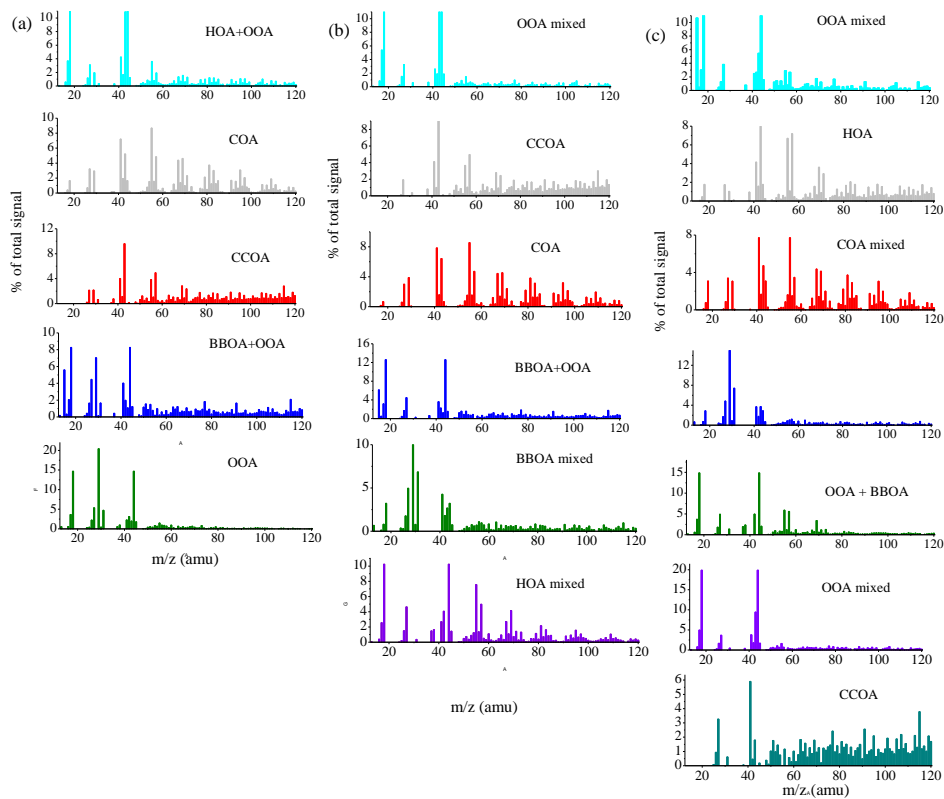
 Figure S2. PMF profiles of OA sources for 5, 6 and 7 factor solutions during winter.
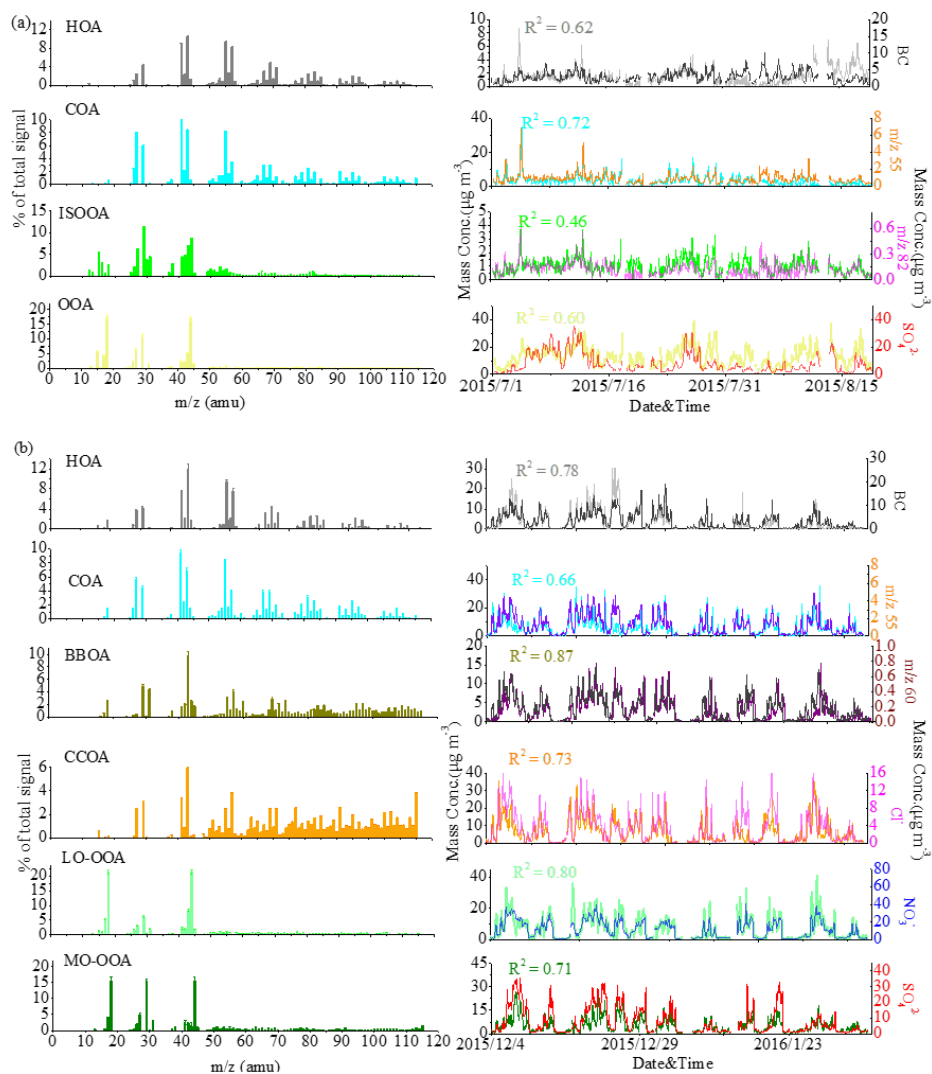
Figure S3. Mass spectrums (left) and time series (right) of OA sources during summer (a) and winter (b). Error bars of mass spectrums represent the standard deviation of each m/z over all accepted solutions.
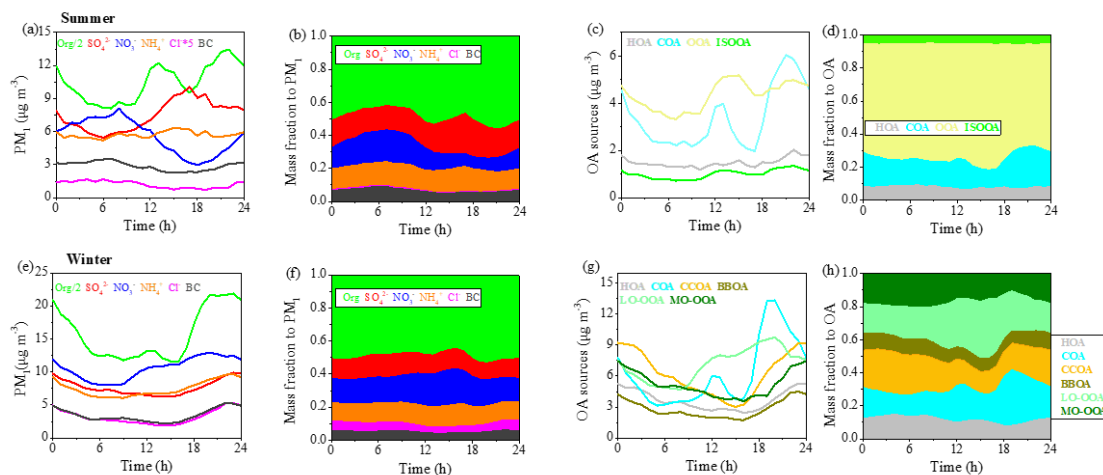
Figure S4. Diurnal variations of mass concentrations and mass fractions of PM$_1$ components and OA sources during summer (a, b, c, d) and winter (e, f, g, h).
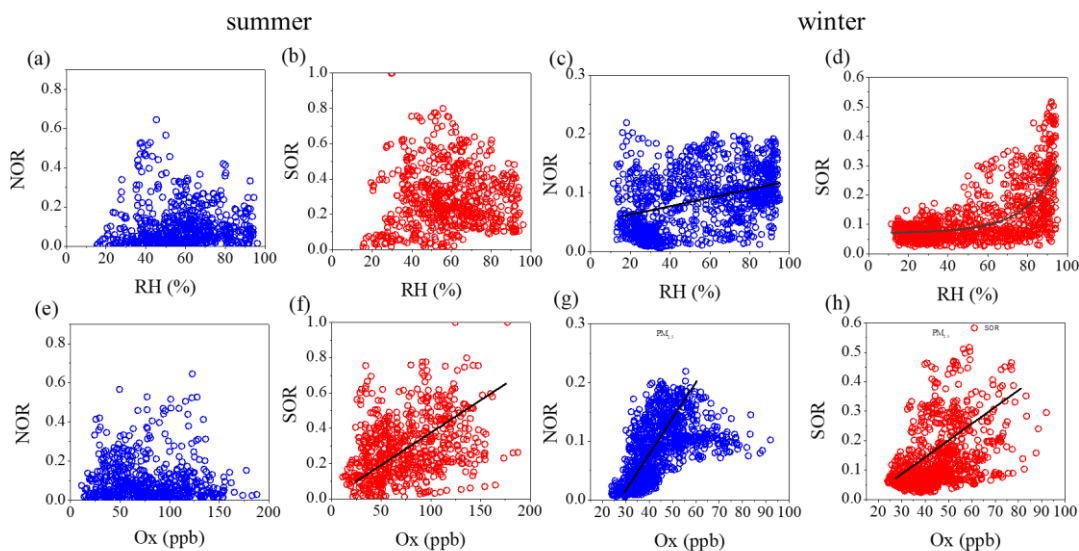
Figure S5. Effects of RH on NOR or SOR during summer (a, b) and winter (c, d), as well as effects of Ox on NOR or SOR during summer (e, f) and winter (g, h).

Reference:

Alfarra, M. R., Prévôt, A. S. H., Szidat, S., Sandradewi, J., Weimer, S., Schreiber, D., Mohr, M., and Baltensperger, U.: Identification of the mass spectral signature of organic aerosols from wood burning emissions, Environ. Sci. Technol., 41(16), 5770–5777, 2007.

Budisulistiorini, S. H., Canagaratna, M. R., Croteau, P. L., Marth, W. J., Baumann, K., Edgerton, E. S., Shaw, S. L., Knipping, E. M., Worsnop, D. R., Jayne, J. T., Gold, A., and Surratt, J. D.: Real-time continuous characterization of secondary organic aerosol derived from isoprene epoxydiols in downtown Atlanta, Georgia, using the Aerodyne Aerosol Chemical Speciation Monitor, Environ. Sci. Technol., 47(11), 5686–5694, 2013.

Canagaratna, M. R., Jayne, J. T., Ghertner, D. A., Herndon, S., Shi, Q., Jimenez, J. L., Silva, P. J., Williams, P, Lanni, T., Drewnick, F., Demerjian, K. L., Kolb, C. E., and Worsnop, D. R.:   Chase studies of particulate emissions from in-use New York City vehicles, Aerosol Sci. Tech., 38, 555–573, 2004.

Crippa, M., Decarlo, P. F., Slowik, J. G., Mohr, C., Heringa, M. F., Chirico, R., Poulain, L., Freutel, F., Sciare, J., Cozic, J., Di Marco, C. F., Elsasser, M., Nicolas, J., Marchand, Nicolas, Abidi, E., Wiedensohler, A., Drewnick, F., Schneider, J., Borrmann, S., Nemitz, E., Zimmermann, R., Jaffrezo, J.-L., Prévôt, A. S. H., and Baltensperger U.: Wintertime aerosol chemical composition and source apportionment of the organic fraction in the metropolitan area of Paris, Atmos. Chem. Phys., 13, 961–981, https://doi.org/10.5194/acp-13-961-2013, 2013.

Dall'Osto, M., Ovadnevaite, J., Ceburnis, D., Martin, D., Healy, R. M., O'Connor, I. P., Kourtchev, I., Sodeau, J. R., Wenger, J. C., and O'Dowd, C.: Characterization of urban aerosol in Cork city (Ireland) using aerosol mass spectrometry, Atmos. Chem. Phys., 13, 4997–5015, https://doi.org/10.5194/acp-13-4997-2013, 2013.

Elser, M., Huang, R. J., Wolf, R., Slowik, J. G., Wang, Q., Canonaco, F., Li, G., Bozzetti, C., Daellenbach, K. R., Huang, Y., Zhang, R., Li, Z., Cao, J., Baltensperger, U., El-Haddad, I., and Prévôt, A. S. H.: New insights into PM2.5 chemical composition and sources in two major cities in China during extreme haze events using aerosol mass spectrometry, Atmos. Chem. Phys., 16, 3207–3225, https://doi.org/10.5194/acp-16-3207-2016, 2016.

Hu, W. W., Hu, M., Yuan, B., Jimenez, J. L., Tang, Q., Peng, J. F., Hu, W., Shao, M., Wang, M., Zheng, L. M., Wu, Y. S., Gong, Z. H., Huang, X. F., and He, L. Y.: Insights on organic aerosol aging and the influence of coal combustion at a regional receptor site of central eastern China, Atmos. Chem. Phys., 13, 10095–10112, https://doi.org/10.5194/acp-13-10095-2013, 2013.

Hu, W. W., Campuzano-Jost, P., Palm, B. B., Day, D. A., Ortega, A. M., Hayes, P. L., Krechmer, J. E., Chen, Q., Kuwata, M., Liu, Y. J., de Sá, S. S., McKinney, K., Martin, S. T., Hu, M., Budisulistiorini, S. H., Riva, M., Surratt, J. D., St. Clair, J. M., Isaacman-Van Wertz, G., Yee, L. D., Goldstein, A. H., Carbone, S., Brito, J., Artaxo, P., de Gouw, J. A., Koss, A., Wisthaler, A., Mikoviny, T., Karl, T., Kaser, L., Jud, W., Hansel, A., Docherty, K. S., Alexander, M. L., Robinson, N. H., Coe, H., Allan, J. D., Canagaratna, M. R., Paulot, F., and Jimenez, J. L.: Characterization of a real-time tracer for isoprene

epoxydiols-derived secondary organic aerosol (IEPOX-SOA) from aerosol mass spectrometer measurements, Atmos. Chem. Phys., 15, 11807–11833, https://doi.org/10.5194/acp-15-11807-2015, 2015.

Hu, W., Hu, M., Hu, W., Jimenez, J. L., Yuan, B., Chen, W., Wang, M., Wu, Y., Chen, C., Wang, Z., Peng, J., Zeng, L., and Shao, M.: Chemical composition, sources, and aging process of submicron aerosols in Beijing: Contrast between summer and winter, J. Geophys. Res. Atmos., 121(4), 1955–1977, https://doi.org/10.1002/2015JD024020, 2016.

Hu, W., Hu, M., Hu, W.-W., Zheng, J., Chen, C., Wu, Y., and Guo, S.: Seasonal variations in high time-resolved chemical compositions, sources, and evolution of atmospheric submicron aerosols in the megacity Beijing, Atmos. Chem. Phys., 17, 9979–10000, https://doi.org/10.5194/acp-17-9979-2017, 2017.

Huang, X. F., He, L. Y., Hu, M., Canagaratna, M. R., Sun, Y., Zhang, Q., Zhu, T., Xue, L., Zeng, L. W., Liu, X. G., Zhang, Y. H., Jayne, J. T., Ng, N. L., and Worsnop, D. R.: Highly time-resolved chemical characterization of atmospheric submicron particles during 2008 Beijing Olympic Games using an Aerodyne High-Resolution Aerosol Mass Spectrometer, Atmos. Chem. Phys., 10, 8933–8945, https://doi.org/10.5194/acp-10-8933-2010, 2010.

Lanz, V. A., Alfarra, M. R., Baltensperger, U., Buchmann, B., Hueglin, C., and Prévôt, A. S. H.: Source apportionment of submicron organic aerosols at an urban site by factor analytical modelling of aerosol mass spectra, Atmos. Chem. Phys., 7, 1503–1522, https://doi.org/10.5194/acp-7-1503-2007, 2007.

Mohr, C., Huffman, J. A., Cubison, M. J., Aiken, A. C., Docherty, K. S., Kimmel, J. R., Ulbrich, I. M., Hannigan, M., and Jimenez, J. L.: Characterization of primary organic aerosol emissions from meat cooking, trash burning, and motor vehicles with High-Resolution Aerosol Mass Spectrometry and comparison with ambient and chamber observations, Environ. Sci. Technol., 43, 2443–2449, 2009.

Mohr, C., DeCarlo, P. F., Heringa, M. F., Chirico, R., Slowik, J. G., Richter, R., Reche, C., Alastuey, A., Querol, X., Seco, R., Peñuelas, J., Jiménez, J. L., Crippa, M., Zimmermann, R., Baltensperger, U., and Prévôt, A. S. H.: Identification and quantification of organic aerosol from cooking and other sources in Barcelona using aerosol mass spectrometer data, Atmos. Chem. Phys., 12, 1649–1665, https://doi.org/10.5194/acp-12-1649-2012, 2012.

Ng, N. L., Canagaratna, M. R., Jimenez, J. L., Zhang, Q., Ulbrich, M., and Worsnop, D. R.: Real-time methods for estimating organic component mass concentrations from aerosol mass spectrometer data, Environ. Sci. Technol., 45, 910–916, https://doi.org/10.1021 /es102951k, 2011.

Sun, J., Zhang, Q., Canagaratna, M. R., Zhang, Y., Ng, N. L., Sun, Y., Jayne, J. T., Zhang, X., Zhang, X., and Worsnop, D. R.: Highly time- and size-resolved characterization of submicron aerosol particles in Beijing using an Aerodyne Aerosol Mass Spectrometer, Atmos. Environ., 44, 131–140, https://doi.org/10.1016/j.atmosenv.2009.03.020, 2010.

Sun, Y. L., Wang, Z. F., Fu, P. Q., Yang, T., Jiang, Q., Dong, H. B., Li, J., and Jia, J. J.: Aerosol composition, sources and processes during wintertime in Beijing, China, Atmos. Chem. Phys., 13, 4577–4592, https://doi.org/10.5194/acp-13-4577-2013, 2013.

Sun, Y. L., Wang, Z. F., Du, W., Zhang, Q., Wang, Q. Q., Fu, P. Q., Pan, X., Li, J., Jayne, J., and Worsnop, D. R.: Long-term real-time measurements of aerosol particle composition in Beijing, China: seasonal variations, meteorological effects, and source analysis, Atmos. Chem. Phys., 15, 10149-10165, https://doi.org/10.5194/acp-15-10149-2015, 2015.

Sun, Y., Du, W., Fu, P., Wang, Q., Li, J., Ge, X., Zhang, Q., Zhu, C., Ren, L., Xu, W., Zhao, J., Han, T., Worsnop, D. R., and Wang, Z.: Primary and secondary aerosols in Beijing in winter: sources, variations and processes, Atmos. Chem. Phys., 16, 8309–8329, https://doi.org/10.5194/acp-16-8309-2016, 2016.

Sun, Y., Xu, W., Zhang, Q., Jiang, Q., Canonaco, F., Prévôt, A. S., Fu, P., Li, J., Jayne, J., Worsnop, D. R., and Wang, Z.: Source apportionment of organic aerosol from two-year highly time-resolved measurements by an aerosol chemical speciation monitor in Beijing, China, Atmos. Chem. Phys., 18(12), 8469–8489, 2018.

Wang, Y. C., Huang, R. J., Ni, H. Y., Chen, Y., Wang, Q. Y., Li, G. H., Tie, X. X., Shen, Z. X., Huang, Y., Liu, S. X., Dong, W. M., Xue, P., Fröhlich, R., Canonaco, F., Elser, M., Daellenbach, K.R., Bozzetti, C., Haddad, EI., and Cao, J. J.: Chemical composition, sources and secondary processes of aerosols in Baoji city of northwest China, Atmos. Environ., 158, 128–137, https://doi.org/10.1016/j.atmosenv.2017.03.026, 2017.

Xu, L., Guo, H., Boyd, C. M., Klein, M., Bougiatioti, A., Cerully, K. M., Hite, J. R., Isaacman-VanWertz, G., Kreisberg, N. M., Knote, C., Olson, K., Koss, A., Goldstein, A. H., Hering, S. V., de Gouw, J., Baumann, K., Lee, S. H., Nenes, A., Weber, R. J., and Ng, N.L.: Effects of anthropogenic emissions on aerosol formation from isoprene and monoterpenes in the southeastern United States, Proc. Natl. Acad. Sci. U.S.A., 112(32), E4506–E4507, 2015.

Zhang, J. K., Sun, Y., Liu, Z. R., Ji, D. S., Hu, B., Liu, Q., and Wang, Y. S.: Characterization of submicron aerosols during a month of serious pollution in Beijing, 2013, Atmos. Chem. Phys., 14, 2887-2903, https://doi.org/10.5194/acp-14-2887-2014, 2014.

Zhang, Y., Sun, J., Zhang, X., Shen, X., Wang, T., and Qin, M.: Seasonal characterization of components and size distributions for submicron aerosols in Beijing, Sci. China Earth Sci., 56, 890–900, https://doi.org/10.1007/s11430-012-4515-z, 2013.

Zhang, Y. J., Tang, L. L., Sun, Y. L., Favez, O., Canonaco, F., Albinet, A., Couvidat, F., Liu, D. T., Jayne, J. T., Wang, Z., Croteau, P. L., Canagaratna, M. R., Zhou, H. C., Prevot, A. S. H., and Worsnop, D.R.: Limited formation of isoprene epoxydiols-derived secondary organic aerosol under NOx-rich environments in Eastern China, Geophys. Res. Lett., 44(4), 2035–2043, https://doi.org/10.1002/2016GL072368, 2017.